1 **Preparation for denitrification and phenotypic diversification at the cusp of**

2 **anoxia; a purpose for N_2O reductase *vis a vis* multiple roles of O_2**

3 Kellermann R[1], Hauge K[1], Tjåland R[1], Thalmann S[2], Bakken LR[1], Bergaust L[1]

4 [1]Norwegian University of Life Sciences, Department of Chemistry, Biotechnology and Food Science, Ås, Norway

5 [2]Luminex, Het Zuiderkruis 1, 5215 MV 's-Hertogenbosch, Netherlands

6

Abstract

8 Adaptation to anoxia by synthesizing a denitrification proteome costs metabolic energy, and the

9 anaerobic respiration conserves less energy per electron than aerobic respiration. This implies a

10 selective advantage of the stringent O_2- repression of denitrification gene transcription, which is

11 found in most denitrifying bacteria. In some bacteria, the metabolic burden of adaptation can be

12 minimized further by phenotypic diversification, colloquially termed *bet-hedging*, where all cells

13 synthesize the N_2O reductase (NosZ) but only a minority synthesizes nitrite reductase (NirS), as

14 demonstrated for the model strain *Paracoccus denitrificans*. We hypothesized that the cells lacking

15 NirS would be entrapped in anoxia, but with the possibility of escape if supplied with O_2 or N_2O.

16 To test this, cells were exposed to gradual O_2-depletion or sudden anoxia, and subsequent spikes

17 of O_2 and N_2O. The synthesis of NirS in single cells was monitored by using an *mCherry-nirS*

18 fusion replacing the native *nirS*, and their growth was detected as dilution of green, fluorescent

19 FITC-stain. We demonstrate anoxic entrapment due to e⁻-acceptor deprivation and show that O_2-

20 spiking leads to *bet-hedging*, while N_2O-spiking promotes NirS synthesis and growth in all cells

21 carrying NosZ. The cells rescued by the N_2O-spike had much lower respiration rates than those

22 rescued by the O_2-spike, however, which could indicate that the well-known autocatalytic

23 synthesis of NirS via NO production requires O_2. Our results bring into relief a fitness advantage

24 of pairing restrictive *nirS* expression with universal NosZ synthesis in energy limited systems.

25

26

27

28

Importance

Denitrifying bacteria have evolved elaborate regulatory networks securing their respiratory metabolism in environments with fluctuating oxygen concentrations. Here, we provide new insight regarding their *bet-hedging* in response to hypoxia, which minimizes their N_2O emissions because all cells express NosZ, reducing N_2O to N_2, while a minority express NirS+Nor, reducing NO_2^- to N_2O. We hypothesized that the cells without Nir were entrapped in anoxia, without energy to synthesize Nir, and that they could be rescued by short spikes of O_2 or N_2O. We confirm such entrapment, the rescue of all cells by an N_2O-spike but only a fraction by an O_2-spike. The results shed light to the role of O_2-repression in *bet-hedging* and generated a novel hypothesis regarding the autocatalytic *nirS*-expression via NO production. Insight into the regulation of denitrification, including *bet-hedging*, holds a clue to understanding, and ultimately curbing, the escalating emissions of N_2O which contributes to anthropogenic climate forcing.

Introduction

In the energy hierarchy of dissimilatory processes, denitrification is second only to aerobic respiration. The four-step process where nitrate (NO_3^-) is reduced to di-nitrogen (N_2) via nitrite (NO_2^-), nitric oxide (NO) and nitrous oxide (N_2O), is driven by the metalloenzymes nitrate- (Nar/Nap), nitrite- (NirK/NirS), nitric oxide- ($c/q/qCu_ANor$) and nitrous oxide- (NosZ I or II) reductase (1-3). Thermodynamics dictate that the reduction of nitrate to N_2 releases 95% of the energy per e^- compared to the reduction of O_2 (4), but canonical denitrification yields only ~60% of the charge separation per electron transported (5, 6). Thus, it makes sense that denitrifiers in general, being facultative anaerobes, strongly favor O_2 as electron acceptor, only switching to reduction of alternative e^- acceptors when conditions become anoxic. This transition is orchestrated by a massive, variably tuned apparatus transcriptionally regulated by O_2 and N-oxide sensing systems, e.g. consisting of Fnr/Crp-type proteins (5). Many denitrifying microorganisms have a truncated denitrification pathway because they lack one or more of the genes coding for the four reductases of the full-fledged pathway (7). However, a truncated pathway may even occur in organisms equipped with all the genes due to repressed gene expression or post-transcriptional interference with the synthesis of functional enzymes (8). These premises give rise to a spectrum of physiological variants (7), with implications for the emission of gaseous intermediates, such as the ozone depleting greenhouse gas N_2O (9, 10).

59   Since the metabolic cost of synthesizing proteins is huge compared to the costs of replicating the

60   genes, organisms need transcriptional regulation that secures protein synthesis only when the

61   enzyme is needed (11). The cost of synthesizing the entire denitrification apparatus is high, as it

62   requires the expression of more than 50 functional and ancillary genes (1). Thus, when anoxia is

63   imminent, denitrifying bacteria face the conundrum of when and whether to make the investment

64   of synthesizing the denitrification proteome. Most denitrifying bacteria are non-fermenting,

65   relying on respiration for generation of ATP, and these organisms must synthesize a minimum of

66   denitrification enzymes before oxygen is depleted to avoid entrapment in anoxia without energy

67   to synthesize such enzymes. To our knowledge, Højberg et al. (12) were the first to demonstrate

68   such entrapment, achieved by inflicting sudden anoxia. This shows that excessively stringent

69   transcriptional oxygen-repression of the denitrification genes implies a risk for entrapment in

70   anoxia. On the other hand, lack of negative regulation, resulting in production of the entire

71   denitrification proteome under high O_2 tension, is wasteful and may reduce fitness. The dilemma

72   is exacerbated by the fact that the organisms cannot sense the future oxygen trajectory of their

73   habitat: the imminent anoxia may initiate a long-lasting anoxic spell, or just a transient depression

74   of oxygen concentration. This dilemma and a compromise manifest in the α-proteobacterium,

75   *Paracoccus denitrificans*. The model organism carries the full set of denitrification genes,

76   encoding Nar and Nap, NirS, cNor and NosZ I, but when aerobic cultures face anoxia, all cells

77   express *nosZ*, while only a minor subpopulation synthesizes NirS (13). This was attributed to FnrP-

78   mediated transcription of *nosZ* under semi-oxic conditions (14), but a low probability of *nir* (+

79   *nor*) transcription in the presence of O_2, accompanied by the requirement for autocatalytic

80   induction by NO (via Nnr) for full expression (15, 16). Hence, *P. denitrificans* displays early

81   induction of *nosZ* but strong repression of *nirS* resulting in phenotypic diversification, colloquially

82   termed *bet-hedging*. This is likely to increase fitness on population level: In mixed communities,

83   expressing *nosZ* enables the cells to scavenge N_2O emitted by others, thus maintaining metabolic

84   activity, and avoiding entrapment in anoxia. Should oxygen return, the cells have limited their

85   investment, but in the event of persistent anoxia, respiration of N_2O should enable them to

86   eventually synthesize a full denitrification proteome.

87   It is reasonable to assume that anoxic entrapment underlies the cell differentiation observed in

88   clonal populations of *P. denitrificans*. Previous experiments where O_2 or N-oxides were introduced

89   to non-differentiated cultures of *P. denitrificans* after prolonged periods of electron acceptor

90   deprivation (hours to days) showed rapid recovery of respiration rates (unpublished data). This
91   indicates that spikes of O_2 would represent a second chance for entrapped cells to synthesize a
92   complete denitrification proteome. The effect of oxygen is two-sided, however, as it modulates
93   transcription (suppressing denitrification) and acts as an e-acceptor, but it is not known to play any
94   additional roles during *de novo* synthesis of N-oxide reductases or ancillary factors. Thus, if the
95   required machinery (NosZ) is present, O_2 should be fully replaceable by N_2O as e- acceptor for
96   establishing a full-fledged denitrification proteome. Unlike O_2, N_2O has no known regulatory role
97   and should thus facilitate *nirS* expression in all cells carrying NosZ. However, this has yet to be
98   explored.

99   A prerequisite for studying entrapment in anoxia is the exposure of aerobic cultures to sudden and
100 complete anoxia, which poses a challenge in liquid cultures, as µM concentrations of O_2 remain
101 after sparging or He-washing (Molstad et al. (17) and subsequent sections). We implemented a
102 procedure for removal of residual O_2 after He-washing, prior to inoculation, using glucose oxidase
103 + catalase (GOX; (18)). Remaining O_2 after GOX treatment was ≤ 10 ppmv in headspace
104 (corresponding to ≤ 0.013 µM in the liquid), resulting in complete anoxic entrapment of
105 aerobically raised cells. We tracked NirS (mCherry-*nirS* fusion replacing native *nirS*) and
106 anaerobic growth (dilution of FITC stain) in single cells in cultures of *P. denitrificans* during
107 anoxic entrapment and spiking with O_2 or N_2O. Besides using fluorescence microscopy, we also
108 established a readout method for the detection of physiological expression levels of NirS in flow
109 cytometry using a high sensitivity CCD camera-based flow cytometer. Cells remained viable
110 during prolonged periods of entrapment and were readily recruited to denitrification when supplied
111 with pulses of O_2, albeit displaying the typical *bet-hedging*. Provision of N_2O led to universal NirS
112 synthesis in entrapped cells carrying NosZ, but with lower initial cell specific NirS activity
113 compared to O_2-spiked cells. Thus, O_2 is replaceable as an e-acceptor during the oxic-anoxic
114 transition, and its conflicting roles make it a less effective facilitator of NirS synthesis than N_2O.
115 However, the comparably weaker induction of *nirS* in N_2O-spiked cells indicate an additional role
116 of oxygen in enhancing *nirS* expression, possibly linked to NO and Nnr.

117

118

Results

The glucose oxidase-catalase system

The glucose oxidase-catalase system (GOX) was tested with respect to kinetics of O_2 removal, inactivation of glucose oxidase, specificity (NO or N_2O scavenging), acidification of medium, and toxicity to anaerobically respiring cells. The O_2 removal capacity of GOX was limited by turnover-dependent inactivation of glucose oxidase, thus near-anoxia (≤ 10 ppmv O_2 in headspace, ≤ 0.013 μM in the liquid) could only be achieved after prior depletion of O_2 by He-washing as described. The GOX reactants did not react with NO or N_2O, did not affect the pH of the medium significantly (GOX-treatment of He-washed, sterile medium reduced the pH by 0.08 ± 0.02 pH-units), and had no adverse physiological effect on anaerobically respiring cells. For details, see Supplemental Item 1 (SI_1).

Flow cytometry for detection of mCherry and FITC fluorescence

Flow cytometry was used in the O_2-spiking experiment to distinguish between active and inactive subpopulations. Cells separated well from background by forward scatter (FSC) and side scatter (SSC) (Fig 1 A). To further exclude coincident events and aggregates we used FSC intensity vs FSC aspect ratio which is a morphometric parameter available on CellStream®. Using the imagery captured by the system's CCD camera and object detection/masking, the software allows for evaluation of the ratio of the minor axis divided by the major axis of an ellipse fitted around the detected objects (Fig 1 B). The Amnis® CellStream® allowed for the detection of weak fluorescence in single bacterial cells (tentative approximation of mCherry-NirS proteins per NirS+ cell, in order of magnitude: 10^3, cell size: 1-2 μm by 0.5-1 μm), thus distinguishing between cells with and without mCherry-NirS in a culture after depletion of O_2. Likewise, growing/non-growing sub-populations in a *bet-hedging* culture could be distinguished by FITC intensity, which is retained in nongrowing cells, but diluted by growth (13). Specificity of the signals and detection sensitivity was assessed using appropriate control samples (Fig 1 C & D).

FIGURE 1

Two main experiments: Entrapment in anoxia and spiking with O_2 or N_2O

The subsequent paragraphs summarize the results of the two experiments gauging NirS expression and anaerobic growth in single cells of *P. denitrificans*: 1) during exposure of aerobic cultures to sudden anoxia and partial- or complete entrapment, followed by O_2 spiking; 2) after N_2O spiking following sudden- or gradual (N-oxide deficient) transition to anoxia.

Experiment 1: Entrapment in anoxia and response to subsequent O_2-spiking

The experiment was designed to secure a fast transition to complete anoxia i.e., rapid depletion of residual O_2, by using a large inoculum. This would entrap a majority of cells in anoxia, based on the theory of a probabilistic initiation of *nirS* transcription in response to hypoxia, and that cells which fail to synthesize NirS before O_2 is depleted will be unable to do so later because they lack the energy (13). According to this theory, 1) a minority of the cells would avoid entrapment in He-washed vials (containing only 450 ppmv O_2 in the headspace), 2) an even lower number of cells (if any) would make it in the vials pretreated with GOX (containing ≤ 10 ppmv O_2) and 3) a subsequent spike of O_2 would enable NirS synthesis in at least a fraction of the cells. The gas kinetics lend strong support to this theory: 1) In the He-washed vials, there was detectable and exponentially increasing N_2-production after depletion of the residual O_2, but the calculated electron flow rates to denitrification indicated that less than 10 % of the cells had switched to anaerobic respiration and growth 2) in the vials pretreated with GOX, N_2 production remained below the system's detection limit throughout the 120 h incubation, 3) a spike of oxygen after 69 h (6 μM in the liquid, depleted within 20-30 h) induced significant N_2 production in the GOX-treated vials after depletion of the oxygen, and resulted in enhanced N_2-production (after O_2-depletion) in the He-washed vials. These phenomena were observed both for unstained and FITC-stained cells. Detailed gas data and electron flow rates for FITC stained and unstained cells are shown in SI_2, and the apparent anaerobic growth rates as calculated by nonlinear regression of the N_2-production rate against time are shown in SI_4.

FITC stained cultures; gas kinetics and flow cytometry

The accumulation of gaseous N-oxides and N_2 and OD_{660} measurements were used to estimate average e- flow rates per cell to denitrification ($v_{e\text{-}dT}$, fmol e$^-$ cell^{-1} h^{-1}) (Fig 2 A). In the He-washed vials untreated by GOX, $v_{e\text{-}dT}$ fluctuated below 0.1 fmol e$^-$ cell^{-1} h^{-1} for 40 h, before gradually increasing, exceeding 1.5 fmol e$^-$ cell^{-1} h^{-1} towards the end of the experiment. Injection of O_2 to

6

177 such vials after 69 h led to transient suppression of $v_{e\text{-}dT}$ followed by a sharp increase to higher

178 levels than in the vials that were not spiked with O_2. The cultures in GOX-treated vials remained

179 largely inactive (except for minimal accumulation of NO and N_2O, SI_2), unless spiked with O_2

180 after 69 h, which induced a subsequent exponential increase in $v_{e\text{-}dT}$, reaching 0.6 fmol cell^{-1} h^{-1} at

181 the end of the experiment (Fig 2 A).

182 The low initial $v_{e\text{-}dT}$, and its increase with time was expected, assuming that a majority of the cells

183 became entrapped in anoxia without NirS, while a minority synthesized NirS in time, sustaining

184 subsequent anaerobic respiration and growth. This was corroborated by inspecting FITC and

185 mCherry-NirS fluorescence in the cells by flow cytometry as shown in Figure 2C. In these plots

186 of mCherry intensity versus FITC intensity, all cells are expected to be in the lower right quadrant

187 initially (no mCherry and high FITC), and as they synthesize mCherry-NirS they move to the upper

188 right quadrant, and if growing, they dilute FITC and move towards the upper left quadrant.

189 In the He-washed vials (not GOX treated) (Vial 1.2 in Figure 2A & C), ~8% of the cells had

190 expressed NirS (mCherry positive) and grown (diluted FITC) after 65 hours, and the fraction

191 increased gradually throughout the rest of the incubation, while a very low fraction resided in the

192 upper right quadrant, i.e., cells that had expressed *nirS* but not grown. In the vial spiked by O_2 after

193 69 hours (Vial 1.3), two NirS-positive populations were detected after 91 hours: one with a very

194 diluted FITC signal and one with a much higher signal. The latter plausibly represents cells that

195 had been entrapped in anoxia but enabled to synthesize NirS due to the O_2-spike. This extra

196 recruitment to denitrification was also seen as an increase in the average cell specific electron flow

197 to denitrification ($v_{e\text{-}dT}$), subsequent to the depletion of the O_2-spike (Vial 1.3 versus Vial 1.2, Fig

198 2A).

199 In the GOX-treated vials without O_2-spiking (Vial 1.8 Fig 2A & C), essentially all cells remained

200 in the lower right quadrant, i.e., without NirS and no growth, indicating that the entire population

201 was entrapped in anoxia without NirS. If spiked with O_2, however (Vial 1.9), a new population

202 emerged with full expression of NirS and with a subsequent gradually declining FITC-signal,

203 indicating growth by anaerobic respiration.

204 In vials without GOX, cumulative cell densities (based on direct counts by flow cytometry

205 corrected for dilution by liquid sampling) correlated well with growing subpopulations of active

206   cells (F_A) (Fig 2B, upper panel). In GOX treated vials, F_A never increased to levels sufficient for
207   any detectable increase in cell density (Fig 2B, lower panel).

208

209   FIGURE 2

210

211   *Estimation of active population in unstained cultures*

212   While flow cytometry provided direct observation of the fraction of actively denitrifying cells
213   (F_A= the fraction of mCherry-positive, FITC diluting cells), F_A can also be estimated from
214   measured gas kinetics and cell density, provided that we know the cell-specific rate of electron
215   flow to denitrification in the active cells = v_{e-dA} (mol e^- cell^{-1}h^{-1}):

216                          $$F_A = \frac{V_{e-D}}{v_{e-dA}*N_T}$$ (1)

217   where V_{e-D} is the measured rate of electron flow to denitrification in the vial (mol e^- vial^{-1} h^{-1}) as
218   calculated from the measured gas kinetics, and N_T is the total number of cells (cells vial^{-1}), as
219   measured by OD. The experiments provide no direct measurements of v_{e-dA}, however, and to
220   estimate this, we fitted (by least square) F_A= (V_{e-D}/v_{e-dA})/N_T (equation 1) to F_A measured by flow
221   cytometry (adjusting v_{e-dA}) with the Generalized Reduced Gradient Solver in Excel, using data
222   from vials 1.2, 1.3, 1.8 and 1.9 (Table 1). The result (Figure 3A) shows a reasonable fit throughout,
223   with v_{e-dA} = 2.5 fmol e^- cell^{-1}h^{-1}. This means that the measured electron flow kinetics could be used
224   to estimate F_A throughout the batch cultivation of unstained cultures, as shown in Fig 3B. This
225   shows that unstained cultures responded similarly to the FITC-stained cells: In the He-washed
226   vials (not GOX treated), recruitment to denitrification was evident immediately after inoculation,
227   followed by a gradually increasing fraction of active cells. The cells in the GOX treated vials
228   remained inactive until spiked with O_2, which induced recruitment to denitrification, and the active
229   fraction subsequently increased to reach ~0.8 (80%) towards the end of the experiment. The
230   apparent growth rates of the active populations in this experiment were estimated by nonlinear
231   regression of the electron flow rates to denitrification against time (Supplementary item 4, Table
232   1), and were 0.038 h^{-1} (se= 0.001 h^{-1}, n=4) for the He washed vials without GOX. (Fig 3B).

233

234 FIGURE 3

235

236 ***Experiment 2: Entrapment in anoxia and response to subsequent N₂O-spiking***

237 In this experiment, aerobically raised, FITC-stained cells either faced sudden anoxia (inoculated

238 to GOX-treated vials) or transient hypoxia (initial O_2 in headspace ~0.25vol%), in a medium that

239 had been stripped for nitrate and nitrite. Nitrite was added 14h after inoculation, i.e., after depletion

240 of O_2. Selected vials were spiked with N_2O or O_2 (Table 1).

241 We hypothesized that cells exposed to sudden anoxia (GOX pretreated vials) would have little or

242 no NosZ, hence they would be unable to utilize a spike of N_2O to generate energy for NirS

243 synthesis. This was verified both by the observed gas kinetics (N_2O was not reduced, and the

244 injection induced no detectable N_2-production from NO_2^-), and by microscopy (no cells expressed

245 NirS, and all retained a high FITC signal). Details are shown in SI 3.

246 In contrast, cells that went through transient hypoxia (initially 0.25 vol% O_2) had evidently

247 synthesized NosZ and were thus poised for NirS synthesis when spiked with N_2O: the N_2O spike

248 was quickly reduced (within ~2h), inducing a subsequent high rate of N_2-production from NO_2^-,

249 and the microscopy revealed that all the cells expressed NirS (became mCherry positive) and grew

250 (diluted the FITC signal) (Figure 4 and Movie 5 & 6; more detailed gas kinetics and microscopy

251 data are shown in SI 3). Prior to the N_2O spiking, however, only a marginal fraction of the cells

252 had synthesized NirS, as evidenced by very low electron flow to denitrification: $v_{e\text{-}dT} < 0.1$ fmol e⁻

253 cell⁻¹ h⁻¹ (Fig 4A), which assuming $v_{e\text{-}dA} = 2.5$ fmol e cell⁻¹ h⁻¹ is equivalent to $F_A < 4\%$.

254 Considering that all cells expressed NirS in response to the N_2O-spike (Fig 4 C, right panel), one

255 would expect that the average electron flow rate per cell ($v_{e\text{-}dT}$) should equal $v_{e\text{-}dA} = 2.5$ fmol cell⁻¹

256 h⁻¹ as determined for the active cells in experiment 1 (see Fig 3). During depletion of the N_2O-

257 spike, $v_{e\text{-}dT}$ was indeed very close to 2.5 fmol cell⁻¹ h⁻¹ (the single high value in Figure 4A), but

258 once the N_2O was depleted, i.e. when the cells were forced to use NO_2^-, average $v_{e\text{-}dT}$ fell to 0.6,

259 increasing gradually to 2.0 fmol cell⁻¹ h⁻¹ during the subsequent 30 h. This suggests that a) all cells

260 had expressed *nosZ* prior to N_2O spiking and b) all cells synthesized a minimum of NirS in

261 response to the spiking, and that the amount of NirS per cell increased gradually thereafter.

262

263   These results demonstrate that O_2 and N_2O are entirely interchangeable as e-acceptors to provide

264   entrapped cells with energy to synthesize NirS. But O_2 was less efficient at the population level

265   than N_2O, plausibly due to its role as a repressor of the transcription of *nirS*. We speculated that

266   O_2 could have a secondary effect on NirS synthesis by dampening the positive feedback via NO,

267   i.e., that O_2 induce a sudden and complete shutdown of NO production and tested this in an

268   additional experiment where actively denitrifying cultures were spiked with N_2O and O_2,

269   monitoring NO and the rate of NO_2^- reduction in response to this spiking. The results lend no

270   support to the hypothesis, however: While V_{eNIR} dropped in response to O_2, the shutdown was

271   complete in response to N_2O but only partial by O_2, and the NO declined to similar levels in

272   response to both (SI 5).

273

274   FIGURE 4

275

276   An alternative explanation to the strong effect of N_2O injection on the synthesis of NirS (Fig 4)

277   could be a regulatory effect of N_2O as such, via an unknown N_2O sensor protein. To test this, we

278   conducted an experiment with a *nosZ* deficient mutant, and the wild type as control, both incubated

279   with- and without 0.4 vol% N_2O in the headspace (~120 µM N_2O in the liquid) and with 0.5 vol%

280   O_2 in the headspace (SI 3, Fig VI). To ensure that most cells became entrapped in anoxia, the

281   cultures were provided with NO_2^- at a time when oxygen was nearly depleted. The measured

282   kinetics of anaerobic respiration was used to estimate the fraction of cells expressing NirS (F_{den}),

283   by fitting a simplified version of the model by Hassan *et al.* (2016). For the wildtype F_{den} increased

284   from 0.01 (± 0.0025) in the cultures without N_2O to 0.13 (± 0.015) in those provided with N_2O. In

285   contrast, F_{den} of the *nosZ* mutant remained low in both treatments: 0.0043 (± 0.0012) without N_2O

286   and 0.0075 (± 0.24) with N_2O (SI 3, Fig VII).

287

288 Discussion

289   We have previously demonstrated that *P. denitrificans* displays phenotypic diversification (*bet-*

290   *hedging*) when preparing for anoxia, i.e., only a fraction of the population expresses *nirS*, but all

291 cells synthesize NosZ (13). Although we had a tentative explanatory model, a refined approach

292 was necessary to understand 1) whether cells that fail to synthesize NirS before O_2-depletion

293 become entrapped in anoxia due to energy deprivation and 2) the efficacy of N_2O- and O_2-spiking

294 in promoting NirS synthesis. We found compelling evidence for anoxic entrapment and a fitness

295 advantage of early NosZ expression, but we also made observations propounding reflections on

296 the roles of O_2 and NO in transcriptional and metabolic regulation of denitrification.

297 The transcriptional regulation of denitrification has been extensively studied (19-21), but the

298 respective roles of the three Fnr-type regulators FnrP, Nnr and NarR and their effectors (O_2 and

299 N-oxides) are still not entirely clear. Part of the explanation for this is the indistinguishable binding

300 sites of the respective factors (22). Oxygen limiting conditions activate FnrP, which positively or

301 negatively regulates the expression of many genes. Among those positively regulated in *P.*

302 *denitrificans* are the cbb$_3$ high affinity oxidase (23), and *nar* and *nos* (24). The *nir* genes have been

303 reported to be subject to negative regulation by FnrP (20), most likely through crosstalk with Nnr.

304 FnrP is found in higher numbers compared to Nnr in *P. denitrificans* (20) and unlike Nnr and

305 NarR, it only requires release from O_2 suppression for its activation. Thus, FnrP constitutes the

306 majority of active Fnr-type proteins in cells facing anoxia and may contribute strongly to (leaky)

307 repression of *nir* expression. Besides repression by FnrP, other O_2 responsive systems may be

308 involved in *nir* regulation, such as the recently described *denR*-NirR system (25). The current

309 wisdom is that in hypoxic cells where *nir* escapes repression, production of a fully functional NirS

310 pool is driven by the positive feedback loop with NO via Nnr and fueled by respiration of the

311 remaining O_2 (16). Of note, the NO signal is subject to quenching by NO scavenging proteins such

312 as the flavohemoglobin Hmp (26) and eventually the respiratory NO reductase, Nor. This could

313 further restrict the initial synthesis of NirS.

314 Denitrification is also regulated at the metabolic level. It is well known that actively denitrifying

315 cells shut down denitrification almost instantaneously if provided with O_2, which was clearly the

316 case in our experiment: spiking with O_2 lowered the denitrification rate to a minimum (Fig 2A),

317 until the concentration of O_2 in the liquid reached <0.5 μM. This response can be ascribed to a

318 competition for electrons between terminal oxidases and the N-oxide reductases, as studied by I.

319 Kucera and V. Sedlacek (27), who found that in *P. denitrificans*, the high affinity *cbb3*-type

320 oxidases played a key role in drawing electrons away from the N-oxide reductases. Our

321 experiments demonstrated (SI 5) that the electron flow is drawn effectively away from NirS by
322 terminal oxidases (in response to O_2-spiking) and even more effectively by N_2O reductase (in
323 response to N_2O-spiking), while the NO concentrations reached similarly low levels by O_2- and
324 N_2O- spiking. This phenomenon has implications for our understanding of NO's role (if any) in
325 the regulatory biology underpinning the *bet-hedging* in *P. denitrificans*.

326 The *bet-hedging* of *P. denitrificans* in response to O_2-depletion has previously been ascribed to a
327 low probability for a cell to initiate *nirS*-transcription (as discussed above), resulting in two
328 populations after oxygen depletion: one actively denitrifying population with NirS, and one
329 entrapped in anoxia without energy for synthesizing NirS (13, 15, 16). Direct evidence for energy-
330 dependent entrapment in anoxia was lacking however, and the role of O_2 as repressor and NO as
331 an inducer of the initial transcription of *nirS* remained unclear. Our results lend strong support to
332 the energy-dependent entrapment, by demonstrating that the entrapped cells could indeed
333 synthesize NirS if provided with a spike of either N_2O or O_2. Further, the fact that all the entrapped
334 cells synthesized NirS in response to the N_2O-spike, while a minority did so in response to the O_2-
335 spike can be taken to illustrate the role O_2-responsive factors as repressors of *nirS* under hypoxia,
336 resulting in a very low probability for a cell to initiate transcription of *nirS*. The role of NO is still
337 elusive, however: In theory, NO could play two roles: one is to secure autocatalytic synthesis of
338 NirS once the first molecules of NirS in a cell become active, producing NO. A second role could
339 be that NO produced by the cells with NirS could induce the initiation of *nirS*-transcription in cells
340 without any NirS. Such signaling does not seem to occur, however. A tentative explanation could
341 be that during the transition to anoxia, such NO signaling is effectively quenched by the NO-
342 scavenging protein Hmp, which is most active under aerobic conditions (26). Under anoxic
343 conditions, Nor is likely the main NO-sink. Whatever causes NO scavenging, the concentration of
344 NO did decline to similarly low levels in response to O_2- and the N_2O spike (SI 5), while *bet
345 hedging* only occurred in response to the O_2-spike.

346 It is tempting to speculate that NO as such is not the inducer of transcription of *nirS*, but that the
347 culprit is one of its possible products within the cell (28). If so, this unknown $^xNO^x$ derived from
348 NO, would be able to secure a positive feedback of *nirS*-transcription within a cell, but plausibly
349 not affect the transcription in other cells if retained within the cell, or that its half-life is too short
350 for it to reach out to other cells. Supposing that the formation of our hypothetic $^xNO^x$ requires O_2,

the positive feedback loop of *nirS*-transcription would not be effective in anoxia, as appeared to be the case in the cultures spiked with N_2O: the cell-specific NirS activity increased gradually throughout a period of 20 h. Peroxynitrite (ONOO⁻/ONOOH, $pK_a= 6.8$) is a compound that could fill these criteria: it is readily formed from NO by a very fast chemical reaction with superoxide (O_2^-) (28), and O_2^- is a by-product of reactions between O_2 and complexes within the e-transport chain. As a result, NO production within a cell will generate peroxynitrite under hypoxia, but less (if any) if oxygen is absent. At cytoplasmic pH, which is typically 7-7.5, peroxynitrite ($pK_A=6.8$) will be predominantly anionic, thus retained within the cell. While highly speculative, this hypothesis is tantalizing because it can explain the observed phenomena which appear to conflict with the conventional concept of NO as the signal molecule sensed by Nnr. Of note, the identification of Nnr as an NO sensor was deduced from *in vivo* experiments, and there is no direct evidence that Nnr reacts directly with NO (22, 29). Ironically, our refined *in vivo* experiments can be taken to suggest that NO is not the substance sensed by Nnr.

Conclusion

We have strong evidence in favor of our longstanding hypothesis that NosZ can act as an energy efficient safety valve in substrate poor systems where oxygen fluctuates. In case of a short-lived anoxic spell, the cells limit their investment by restrictive NirS production but secures the option of continued respiration and growth through scavenging N_2O emitted by the surrounding microbial community. As such, NosZ provides a second chance to cells which initially "opted out" of full-fledged denitrification, e.g., the energy to eventually produce the complete set of denitrification proteins. In addition to this insight into the fitness advantage of *bet-hedging*, a novel understanding of the role of oxygen *vis á vis* the autocatalytic regulation of NirS is emerging. This multiplicity, where oxygen is concurrently suppressor, e⁻ acceptor and enhancer of gene expression speaks to the intricacy of the denitrification regulatory network, and it will fuel further enquiries into the interplay between NO and reactive oxygen species.

Acknowledgements

13

Materials and Methods

Organism

All experiments were performed on *P. denitrificans* Pd1222 where an *mCherry-nirS* fusion gene replaces the native *nirS* gene, which allows the tracking of NirS in individual cells by fluorescence microscopy [13]. For testing the potential regulatory effect of N_2O Pd1222 wild type and a *nosZ* mutant derived from this strain were used [20].

Medium

Sistrom's medium as described by Lueking et al. [30] with 34 mM succinate, pH=7 was used throughout and KNO_2 (1 or 2 mM) was added as e$^-$ acceptor for anoxic respiration. For experiments where complete absence of nitrate and nitrite was essential, we stripped the medium for these nitrogen oxyanions prior to use, as described in detail by Bergaust et al. [24]. In short, the stripping was achieved by anaerobic incubation of medium with ~10^7 *Paracoccus denitrificans* cells mL^{-1}, followed by filtration and autoclaving.

Helium washing

In preparation for incubation experiments, 120 mL serum vials filled with 50 mL Sistrom's medium and a magnetic Teflon stirring bar were sealed with butyl rubber septa and aluminum crimp caps and washed with helium repeatedly: 7 cycles of evacuation followed by filling with helium, using an automated system described by Molstad et al. [17]. This fails to remove all O_2, however, and the O_2 concentration increase gradually during the first 10-20 hours after He-washing due to release of O_2 (and N_2) from the Teflon magnet and the septum [17], stabilizing at 200-400 ppmv (0.6 μM in the liquid) after 20 hours. The standard procedure is thus to He-wash the vials >24 hours before inoculating the vials. The He-washing leaves an overpressure in the vials, and this is released to reach 1 atmosphere after temperature equilibration in the water-bath, by piercing the septum with a syringe filled with 70% ethanol (no piston).

Glucose oxidation treatment (GOX) for removal of residual O_2

To obtain completely anoxic conditions, the residual O_2 in He-washed vials was removed by glucose oxidase+catalase, as described by Thorndycroft et al. [18]. This was done by injecting 1 mL of the mixture of the two enzymes (200 u/mL glucose oxidase, 1000 u/mL catalase), and subsequently 1 mL glucose solution (800 mM glucose) to each vial with 50 mL medium. The

408   efficiency of the GOX treatment was tested thoroughly, including vials with different initial O_2

409   concentrations 1-21 vol% in the headspace, to determine the oxygen scavenging kinetics and the

410   decay rate of the enzymes. We also tested if GOX had any effect on NO and N_2O, by treating vials

411   with these gases in the headspace. Since H_2O_2 is an intermediate in the glucose oxidase + catalase

412   reaction, a transient accumulation of H_2O_2 during O_2 depletion could theoretically have some toxic

413   effects. To avoid this, the vials were GOX-treated 1 day before being inoculated. We tested if this

414   pretreatment with GOX left any residual physiological effect by inoculating vials (untreated and

415   GOX treated) with anaerobically raised cells of *P. denitrificans*.

FITC staining

417   Aerobically raised cells were harvested by centrifugation at 4°C and stained with fluorescein

418   isothiocyanate (FITC) as previously described by Lycus et al. (13). Briefly, cells were incubated

419   with 0.1 mg/mL FITC for 10 min at 4°C and dispersed by pumping through a 0.5 mm needle to

420   ensure the even uptake of the stain. Excess stain was removed by washing the cells three times

421   with 30 mL Sistrom's medium that was nitrite and nitrate free if required.

Incubation and monitoring of gas kinetics

423   Incubations were carried out in a water bath at 17°C if not specified otherwise. Helium washed

424   vials were placed in the incubation system described by Molstad et al. (17). The concentrations of

425   gases in the headspace (O_2, CO_2, NO, N_2O and N_2) were monitored by repeated sampling through

426   the rubber septum. The gas was sampled with a peristaltic pump that returned an equal amount of

427   He to the headspace, ensuring a constant pressure. The dilution of headspace gases by He was

428   accounted for in data analysis. The autosampler is coupled to a chemiluminescence NO/NO_x

429   analyzer (Teledyne 200E) and a GC (Agilent GC-7890A) with a PLOT column for separation of

430   CH_4, CO_2 and N_2O and a Molsieve for separating O_2 and N_2. The GC has a flame ionization (FID),

431   a thermal conductivity (TCD) and an electron capture (ECD) detector. N_2O is detected by both

432   ECD and TCD to ensure accurate measurements at both near-ambient (ECD) and higher

433   concentrations. Continuous stirring at 600 rpm ensured near equilibrium between gas

434   concentrations in liquid and headspace.

Analyses of cell specific electron flow rates to denitrification

436   Given the fact that the cultures were provided with NO_2^- (not NO_3^-), and that the incubation system

437   provided frequent measurements of NO, N_2O and N_2, thus monitoring all reduction steps, the

438 electron flow rate to denitrification could be calculated for each time increment between two gas

439 samplings (V_{e-D}, mol e⁻ vial⁻¹ h⁻¹). For each time increment, we could also estimate the average

440 electron flow rate per cell $v_{e-dT} = V_{e-D}/N_T$, where N_T is the total number of cells in the vial, estimated

441 from measured optical density (OD_{660}). OD was measured with lower frequency than the gas

442 measurements, but by interpolating with the SRS1 cubic spline function (SI 4), we could estimate

443 N_T for each time interval between two gas samplings. Assuming that the cell specific electron flow

444 to denitrification in active cells, v_{e-dA} is known, we have that the fraction of active cells within the

445 whole population of cells, $F_A = v_{e-dT}/v_{e-dA}$. No direct measurements of v_{e-dA} could be made, but

446 estimates were obtained by fitting $F_A = v_{e-dT}/v_{e-dA}$ to F_A as measured by flow cytometry.

447 **Liquid sampling**

448 Liquid samples (3 mL) were taken intermittently during incubations for measurement of OD_{660},

449 and analyses by microscopy or flow cytometry. The bottles were briefly inverted, and the samples

450 were taken through the septum with a syringe. To secure constant liquid volume throughout, an

451 equal volume of He-washed Sistroms medium was injected immediately prior to sampling. The

452 OD_{660} of the sample was measured, and 1.8 mL sample was fixed by adding 38% formalin to a

453 final concentration of 4% pending flow cytometry or microscopy.

454 **Flow cytometry**

455 Formalin fixed samples were diluted to 10^6 cells/mL with filtered (0.1 μm) MilliQ water before

456 loading into the flow cytometer (Amnis® CellStream®, Luminex®). The system was run at slow

457 speed. Laser powers were adjusted to 20% for forward scatter (FSC), 50% for side scatter (SSC),

458 100 % for 488 nm, and 100 % for 561 nm. FSC, SSC and FITC intensity was measured using the

459 528/46 filter, and mCherry intensity was detected using the 611/31 channel. Gating was applied to

460 specify the single bacteria and distinguish between active (mCherry positive, diluting FITC) and

461 inactive (mCherry negative, retaining FITC) subpopulations.

462 **Fluorescence Microscopy**

463 Formalin fixed samples were washed three times with phosphate buffered saline (PBS; 137 mM

464 NaCl, 2.7 mM KCl, 10 mM Na_2HPO_4, 1.8 mM KH_2PO_4, pH = 7), and inspected with fluorescence

465 microscopy, using a Zeiss AxioObserver with ZEN Blue software. The UV exposure times were

466 1000 ms for mCherry and 750 ms for FITC and a HXP 120 Illuminator (Zeiss) was used as the

467 fluorescence UV light source. Images were acquired with an ORCA-Flash4.0 V2 Digital CMOS

468   camera (Hamamatsu Photonics) and images were analyzed using the ImageJ plugin MicrobeJ (31).

469   Cell outlines were detected in the phase contrast images and the FITC and mCherry signal

470   intensities of each cell were determined in the corresponding fluorescent images (13).

471

Two main experiments: Anoxic entrapment and the effect of spiking with O_2 or N_2O

473   *1. O_2 spiking*

474   Vials with 50 mL Sistroms medium without NO_2^- or NO_3^- were inoculated with $\sim 4*10^9$ cells that

475   had been raised under strict aerobic conditions to secure absence of any denitrification enzymes.

476   Prior to inoculation, the vials were either He-washed (2-400 ppmv residual O_2 in the headspace)

477   or He-washed + GOX-treated (completely anoxic), and NO_2^- was injected after 5 hours. The

478   purpose of these treatments was to inspect the effect of exposing cells to sudden anoxia (without

479   NO_2^-) on their ability to express denitrification enzymes. Some vials were inoculated with FITC-

480   stained cells, allowing the distinction between growing and non-growing cells. Others were

481   inoculated with equal amounts of unstained cells, to check if FITC staining would influence the

482   respiration kinetics. Spikes of O_2 (~ 15 µmol $= 350$ µL vial^{-1} or ~ 7.35 µM in liquid) were injected

483   to some vials after 69 h, to assess the capacity of cells that were apparently entrapped in anoxia

484   (without mCherry, retained FITC-stain). Table 1 summarizes the various treatments.

485   Flow cytometry was used to discriminate between active and inactive cells, based on red and green

486   fluorescence as described above.

487   *2. N_2O spiking*

488   Since normal Sistrom's medium contains traces of NO_3^-, which was suspected to influence the

489   percent of cells expressing denitrification enzymes in the first experiment, we used Sistrom's

490   which had been stripped for NO_2^- and NO_3^- in the second experiment. Vials were either completely

491   anoxic (He-washed+GOX-treated) or provided with 0.25 vol% O_2 in headspace prior to

492   inoculation with $\sim 3*10^9$ cells vial^{-1} (aerobically raised, FITC stained). NO_2^- was injected (100

493   µmol vial^{-1}) after 14 h, when the vials with 0.25 vol% O_2 had become completely anoxic. During

494   the anoxic phase of the incubation, vials were spiked with either ~ 15 µmol O_2 or ~ 20 µmol N_2O

495   (250 µL vial^{-1}; ~ 77 µM in liquid). The amount of O_2 injected during the spiking experiments was

496   chosen based on previous observations of maximal *nirS* (+ *norB*) transcription at $O_2 < 15$ µM in

497   liquid (14), thus ensuring provision of electron acceptor, while avoiding severe suppression of *nir*

498   and *nor* expression. The amount of N_2O was selected to ensure adequate provision of electron

499   acceptor, albeit for a shorter time window compared to the oxygen spike. Table 1 summarizes the

500   treatment of the individual vials.

501   Presence of NirS (mCherry, red fluorescence) and growth (dilution of FITC stain, green

502   fluorescence) in single cells was monitored in selected liquid samples by fluorescence microscopy

503   and image analysis as described above and in Lycus et al. (13).

504

505   TABLE 1

506

Data availability

508   Raw data from gas measurements, microscopy and flow cytometry can be made available upon

509   request.

510   Supporting information referred to in the paper thoroughly describes the data and the analyses, and

511   is found at https://data.mendeley.com/: Bergaust, Linda (2022), "Kellermann et al

512   2022_Preparation for denitrification at the cusp of anoxia", Mendeley Data, V3, doi:

513   10.17632/zpwkwwg5xz.3

514   **Movie 1-6:** Red (mCherry-NirS expression) and green (FITC, growth) fluorescence in single cells

515   captured by flow cytometry (Movie 1-4; O_2-spiking experiment) or fluorescence microscopy and

516   image analyses (Movie 5-6; N_2O spiking experiment). Movie 1: vial 1.2; Movie 2: vial 1.3; Movie

517   3: vial 1.8; Movie 4: vial 1.9; Movie 5: vial 2.3 and 2.4; Movie 6: vial 2.7 and 2.11.

518   **Supplemental items (SI) 1-5**: Supplemental item 1 is a description and qualification of the glucose

519   oxidase-catalase (GOX) approach used for the removal of residual oxygen in experimental vials

520   before inoculation. In supplemental item 2, we display the gas- and flow cytometry data in the O_2

521   spiking experiment, including the data shown in Figure 2 and 3 in the paper. In supplemental item

522   3, we show the gas kinetics and microscopy analyses from the N_2O spiking experiment, which in

523 the paper is summarized in Fig 4. We also show the lack of positive effect from N_2O addition on

524 Nir expression in a NosZ deficient mutant. In supplemental item 4, we describe the steps taken to

525 estimate apparent specific growth rates in single vials and cell yield per mol electron to N-oxides.

526 In supplemental item 5, we describe a simple experiment where nitrite reducing cultures of

527 *Paracoccus denitrificans* was spiked with N_2O and O_2 and the subsequent rate of nitrite reduction

528 was assessed.

529

References

531 1.   Zumft WG. 1997. Cell biology and molecular basis of denitrification. Microbiol Mol Biol
532   Rev 61:533-616.
533 2.   Suharti HAH, Heering HA, de Vries S. 2004. NO reductase from Bacillus azotoformans is
534   a bifunctional enzyme accepting electrons from menaquinol and a specific endogenous
535   membrane-bound cytochrome c551. Biochemistry 43:13487-95.
536 3.   Pauleta SR, Dell'Acqua S, Moura I. 2013. Nitrous oxide reductase. Coord Chem Rev
537   257:332-349.
538 4.   Thauer RK, Jungermann K, Decker K. 1977. Energy conservation in chemotrophic
539   anaerobic bacteria. Bacteriol Rev 41:100-80.
540 5.   van Spanning RJM, Richardson DJ, Ferguson SJ. 2007. Introduction to the biochemistry
541   and molecular biology of denitrification, p 3-20, Biology of the nitrogen cycle. Elsevier.
542 6.   Nicholls D, Ferguson SJL-NY. 2002. Bioenergetics, Academic Press.
543 7.   Lycus P, Lovise Bothun K, Bergaust L, Peele Shapleigh J, Reier Bakken L, Frostegard A.
544   2017. Phenotypic and genotypic richness of denitrifiers revealed by a novel isolation
545   strategy. ISME J 11:2219-2232.
546 8.   Bergaust L, Mao Y, Bakken LR, Frostegard A. 2010. Denitrification response patterns
547   during the transition to anoxic respiration and posttranscriptional effects of suboptimal pH
548   on nitrous [corrected] oxide reductase in Paracoccus denitrificans. Appl Environ Microbiol
549   76:6387-96.
550 9.   Schlesinger WH. 2009. On the fate of anthropogenic nitrogen. Proc Natl Acad Sci U S A
551   106:203-208.
552 10.   Ravishankara A, Daniel JS, Portmann RW. 2009. Nitrous oxide (N2O): the dominant
553   ozone-depleting substance emitted in the 21st century. Science 326:123-125.
554 11.   Lynch M, Marinov GK. 2015. The bioenergetic costs of a gene. Proc Natl Acad Sci USA
555   112:15690-15695.
556 12.   Hojberg O, Binnerup SJ, Sorensen J. 1997. Growth of silicone-immobilized bacteria on
557   polycarbonate membrane filters, a technique to study microcolony formation under
558   anaerobic conditions. Appl Environ Microbiol 63:2920-4.
559 13.   Lycus P, Soriano-Laguna MJ, Kjos M, Richardson DJ, Gates AJ, Milligan DA, Frostegard
560   A, Bergaust L, Bakken LR. 2018. A bet-hedging strategy for denitrifying bacteria curtails
561   their release of N2O. Proc Natl Acad Sci U S A 115:11820-11825.
562 14.   Qu Z, Bakken LR, Molstad L, Frostegard A, Bergaust LL. 2016. Transcriptional and
563   metabolic regulation of denitrification in Paracoccus denitrificans allows low but

564 significant activity of nitrous oxide reductase under oxic conditions. Environ Microbiol
565 18:2951-63.

15. Hassan J, Bergaust LL, Molstad L, de Vries S, Bakken LR. 2016. Homeostatic control of
567 nitric oxide (NO) at nanomolar concentrations in denitrifying bacteria - modelling and
568 experimental determination of NO reductase kinetics in vivo in Paracoccus denitrificans.
569 Environ Microbiol 18:2964-78.

16. Hassan J, Bergaust LL, Wheat ID, Bakken LR. 2014. Low probability of initiating nirS
571 transcription explains observed gas kinetics and growth of bacteria switching from aerobic
572 respiration to denitrification. PLoS Comput Biol 10:e1003933.

17. Molstad L, Dorsch P, Bakken LR. 2007. Robotized incubation system for monitoring gases
574 (O2, NO, N2O N2) in denitrifying cultures. J Microbiol Methods 71:202-11.

18. Thorndycroft FH, Butland G, Richardson DJ, Watmough NJ. 2007. A new assay for nitric
576 oxide reductase reveals two conserved glutamate residues form the entrance to a proton-
577 conducting channel in the bacterial enzyme. Biochem J 401:111-119.

19. Bouchal P, Struharova I, Budinska E, Sedo O, Vyhlidalova T, Zdrahal Z, van Spanning R,
579 Kucera I. 2010. Unraveling an FNR based regulatory circuit in Paracoccus denitrificans
580 using a proteomics-based approach. Biochim Biophys Acta 1804:1350-1358.

20. Giannopoulos G, Sullivan MJ, Hartop KR, Rowley G, Gates AJ, Watmough NJ,
582 Richardson DJ. 2017. Tuning the modular Paracoccus denitrificans respirome to adapt
583 from aerobic respiration to anaerobic denitrification. Environ Microbiol 19:4953-4964.

21. Olaya-Abril A, Hidalgo-Carrillo J, Luque-Almagro VM, Fuentes-Almagro C, Urbano FJ,
585 Moreno-Vivian C, Richardson DJ, Roldan MD. 2018. Exploring the denitrification
586 proteome of Paracoccus denitrificans PD1222. Front Microbiol 9:1137.

22. Spiro S. 2016. Regulation of denitrification, p 312-30. *In* Isabel Moura JJGM, Sofia R.
588 Pauleta, Luisa B. Maia (ed), Metalloenzymes in denitrification: applications

589 environmental impacts. Royal Society of Chemistry, London.

23. Otten MF, Stork DM, Reijnders WN, Westerhoff HV, Van Spanning RJ. 2001. Regulation
591 of expression of terminal oxidases in Paracoccus denitrificans. Eur J Biochem 268:2486-
592 97.

24. Bergaust L, van Spanning RJ, Frostegard A, Bakken LR. 2012. Expression of nitrous oxide
594 reductase in Paracoccus denitrificans is regulated by oxygen and nitric oxide through FnrP
595 and NNR. Microbiology 158:826-34.

25. Gaimster H, Hews CL, Griffiths R, Soriano-Laguna MJ, Alston M, Richardson DJ, Gates
597 AJ, Rowley G. 2019. A central small RNA regulatory circuit controlling bacterial
598 denitrification and N2O emissions. MBio 10.

26. Hartop KR, Sullivan MJ, Giannopoulos G, Gates AJ, Bond PL, Yuan Z, Clarke TA,
600 Rowley G, Richardson DJ. 2017. The metabolic impact of extracellular nitrite on aerobic
601 metabolism of Paracoccus denitrificans. Water Res 113:207-214.

27. Kucera I, Sedlacek V. 2020. Involvement of the cbb3-Type Terminal Oxidase in Growth
603 Competition of Bacteria, Biofilm Formation, and in Switching between Denitrification and
604 Aerobic Respiration. Microorganisms 8.

28. Bowman LA, McLean S, Poole RK, Fukuto JM. 2011. The diversity of microbial responses
606 to nitric oxide and agents of nitrosative stress: close cousins but not identical twins. Adv
607 Microb Physiol 59:135-219.

29. Spiro S. 2007. Regulators of bacterial responses to nitric oxide. FEMS Microbiol Rev
609 31:193-211.

610   30.   Lueking DR, Fraley RT, Kaplan S. 1978. Intracytoplasmic membrane synthesis in
611   synchronous cell populations of Rhodopseudomonas sphaeroides. Fate of "old" and "new"
612   membrane. J Biol Chem 253:451-7.
613   31.   Ducret A, Quardokus EM, Brun YV. 2016. MicrobeJ, a tool for high throughput bacterial
614   cell detection and quantitative analysis. Nat Microbiol 1:16077.

615

616

617

618

619

620

621

622

623

624

625

626

627

628

629

630

631

632

633

634

Table and figure legends

Table 1: Treatment of individual vials in main experiments. <u>Experiment 1, O_2-spiking</u>: 18 vials with 50 mL Sistrom's medium were either only helium washed (i.e. with 2-400 ppmv O_2) or made completely anoxic by the GOX pretreatment, and inoculated either with unstained cells (n=9) or cells stained with FITC (n=9). KNO_2 (100 μmol vial^{-1}) was after 5 h. In an additional experiment, KNO_2 was added immediately after inoculation, without any consequences for the results (SI 2, Figs IV & V versus VI & VII).   A spike of O_2 (15.5 μmol O_2) was added to selected vials after 69 hours. <u>Experiment 2, N_2O-spiking:</u> 23 vials with Sistrom's medium that had been stripped of nitrite and nitrate, either completely anoxic (pretreated with GOX, n=12) or with 0.25 vol% O_2 in the headspace (n=11), were all inoculated with FITC stained cells. 100 μmol KNO_2 was injected after 14 h. Selected vials were spiked with either O_2 or N_2O. <u>Both experiments:</u> Liquid sampling for OD measurement, microscopy (Exp. 2) and flow cytometry (Exp. 1), was made throughout in some vials, while others were left untouched to obtain undisturbed measurement of the gas kinetics. Light red shading indicates vials for which results are reported within supplementary items only.

Figure 1: Gating strategy and detection of mCherry and FITC. Panel A: Discrimination of bacterial population from background noise in FSC-456/51 vs SSC-773/56 scatter plot (20 000 observations). Panel B: Identification of singlets within the bacterial population, FSC-456/51 vs Aspect ratio_FSC-456/51. Panel C: Distribution of FITC fluorescence intensity within the singlet population of an unstained culture (FITC -, grey), stained aerobic inoculum (FITC +, blue), and *bet-hedging* population treated similarly to vial 1.2 in table 1 (red). Panel D: Distribution of mCherry fluorescence intensity within singlet population of an aerobic (mCherry negative) culture (mC -, blue), a *bet-hedging* culture (green), and a near 100% NirS positive control that was grown anaerobically over several batches (mC +, red).

Figure 2: Entrapment in anoxia and subsequent recruitment of cells to denitrification by O_2-spiking. Observed activity (gas kinetics) and discrimination of active and inactive subpopulation by flow cytometry in FITC stained *P. denitrificans* at selected timepoints. Complete flow cytometry data are found within supplementary item 2. **Panel A**: Electron flow rate per cell in the total population ($v_{e-dT} = V_{e-D}/N_T$, where V_{e-D} is the electron flow rate to denitrification (mol e$^-$ vial^{-1} h^{-1}) and N_T is the total number of cells in the vial), plotted against time for four different treatments (Table 1); 1.2: He-washed vials, 1.3: He washed vials spiked with O_2 after 69 h, 1.8:

22

665 completely anoxic vials (GOX pretreated) and 1.9: completely anoxic vials spiked with O_2 after
666 69 h. The oxygen spike is shown as a shaded area (complete data in SI 2). **Panel B:** Cumulative
667 cells mL^{-1}, and the fraction of actively denitrifying cells as observed by flow cytometry (population
668 "A", upper, left quadrant, panels C). **Panels C**: Upper two rows show He-washed (not GOX treated
669 vials; 1.2 and 1.3 in panel A) lower two rows show GOX-treated cultures with- and without O_2
670 spiking (1.8 and 1.9 in Panel A). Complete flow cytometry data are shown in Movies 1-4 and in
671 SI 2.

672 **Figure 3: Fraction of active cells (F_A) in unstained cultures. Panel A:** Fraction of active cells
673 (F_A) throughout the incubation of FITC-stained cells estimated by measured electron flow rates
674 (equation 1), fitted by least squares to F_A measured by flow cytometry. The fitting resulted in an
675 estimated cell specific electron flow rate, v_{e-dA} = 2.5 fmol e^- $cell^{-1}$ h^{-1} in active cells. **Panel B:** F_A
676 in unstained cultures throughout the incubations, calculated by equation 1, assuming v_{e-dA} = 2.5
677 fmol e^-cell^{-1} h^{-1}. Open black circles: He washed vials (not GOX treated), n = 2 replicate vials) with-
678 and without O_2 spiking; Open red circles: GOX treated vials (n=2 replicate vials) without O_2
679 spiking; Closed red circles: GOX treated cultures (n=2) spiked with O_2 at 69 h.

680 **Figure 4: Effect of N_2O spiking on NirS synthesis and activity in cells carrying NosZ.** Vials
681 (n = 11) with nitrite/nitrate free medium and 0.25% O_2 in headspace inoculated with FITC stained
682 aerobic cells. 7 vials were spiked with 20 µmol N_2O after ~26 h. **Panel A:** average electron flow
683 to N-oxides (v_{e-dT}, fmol e^- $cell^{-1}$ h^{-1}) during ~50 h of anoxia in cultures with- (red circles) and
684 without (black open circles) N_2O-spiking (grey area). v_{e-dT} is the electron flow rate per cell = V_{e-D}/N_T, where V_{e-D} is the electron flow rate in the whole vial (mol e^- h^{-1}) for each time increment
686 between two gas samplings, and N_T is the cell number per vial for the same time interval. **Panel
687 B:** FITC and mCherry fluorescence in single cells after 27 and 73 h, in vials spiked with N_2O (top
688 panel) and vials not spiked (lower panel). Time resolved development of subpopulations is
689 summarized in Movie 5 & 6. **Panels C:** Fraction of total population carrying mCherry-NirS (as
690 observed by fluorescence microscopy; diamonds) compared to fraction of actively denitrifying
691 cells (F_A; lines) as estimated based on measured electron flow rates and equation (1), assuming
692 that the electron flow rate per active cell v_{e-dA} = 2.5 fmol e- $cell^{-1}$ h^{-1}, as determined previously for
693 oxygen-spiked cells (Fig 3).

694

695 **Table 1**

696

Experiment 1, O$_2$ spiking (Nitrite added after 5 h)				Experiment 2, N$_2$O spiking (all FITC stained, nitrite addition at 14 h)		
Helium washed				**Initially 0.25vol% O$_2$**		
Vial #	**FITC**	**Gas spikes**	**Liquid sampling**	**Vial #**	**Gas spikes**	**Liquid sampling**
1.1	+			2.1-2		
1.2	+		+	2.3-4		+
1.3	+	O$_2$	+	2.5-8	N$_2$O	
1.4				2.9-11	N$_2$O	+
1.5			+			
1.6		O$_2$	+			
GOX pretreated				**GOX pretreated**		
	FITC	**Gas spikes**	**Liquid sampling**		**Gas spikes**	**Liquid sampling**
1.7	+			2.12-13		
1.8	+		+	2.14-15		+
1.9	+	O$_2$	+	2.16-17	N$_2$O	+/-
1.10				2.18-19	N$_2$O + O$_2$	+/-
1.11			+	2.20-21	O$_2$	+/-
1.12		O$_2$	+	2.22-23	O$_2$ + N$_2$O	+/-

697

698

699

700

701

702

703

704
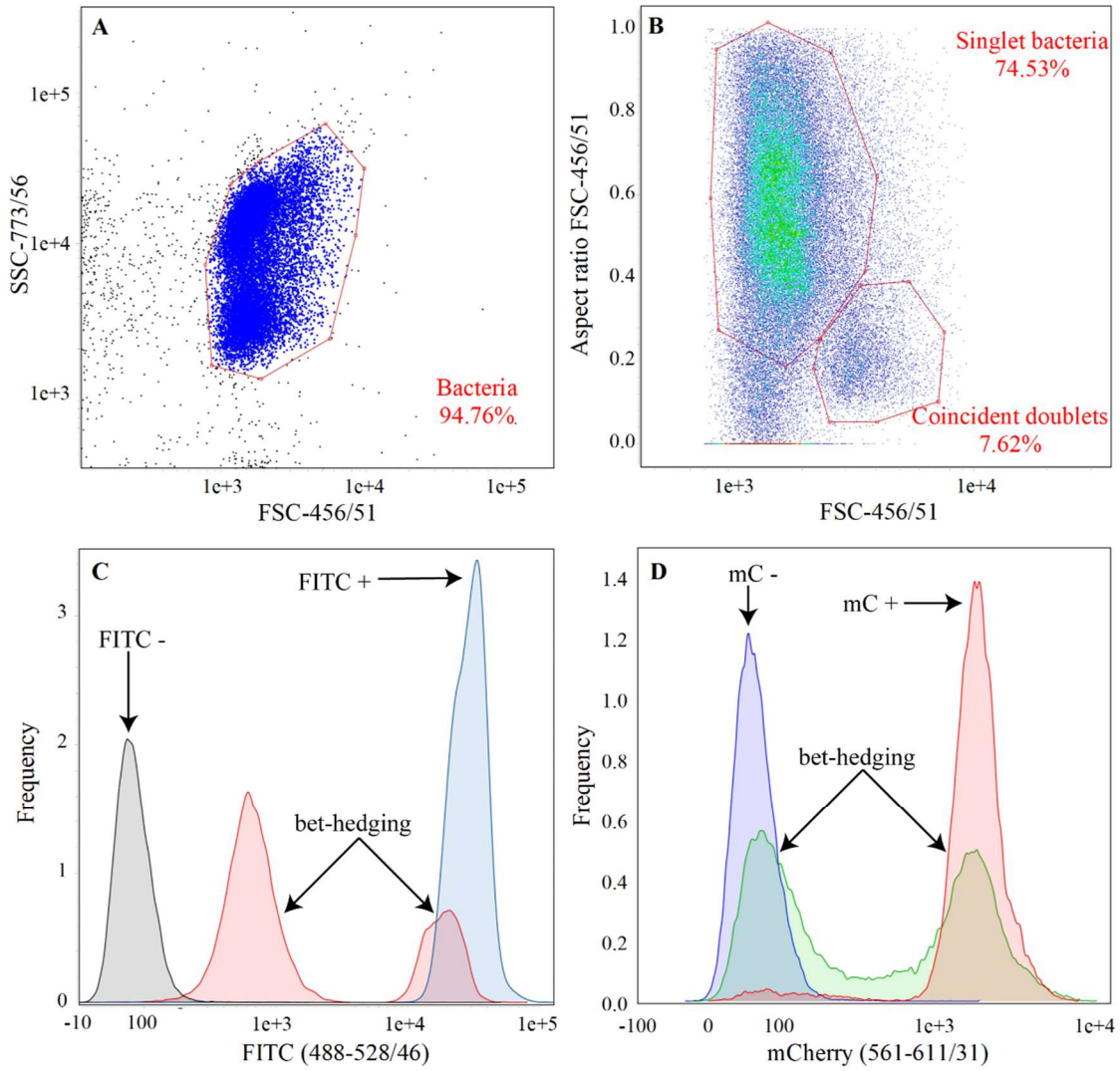
705
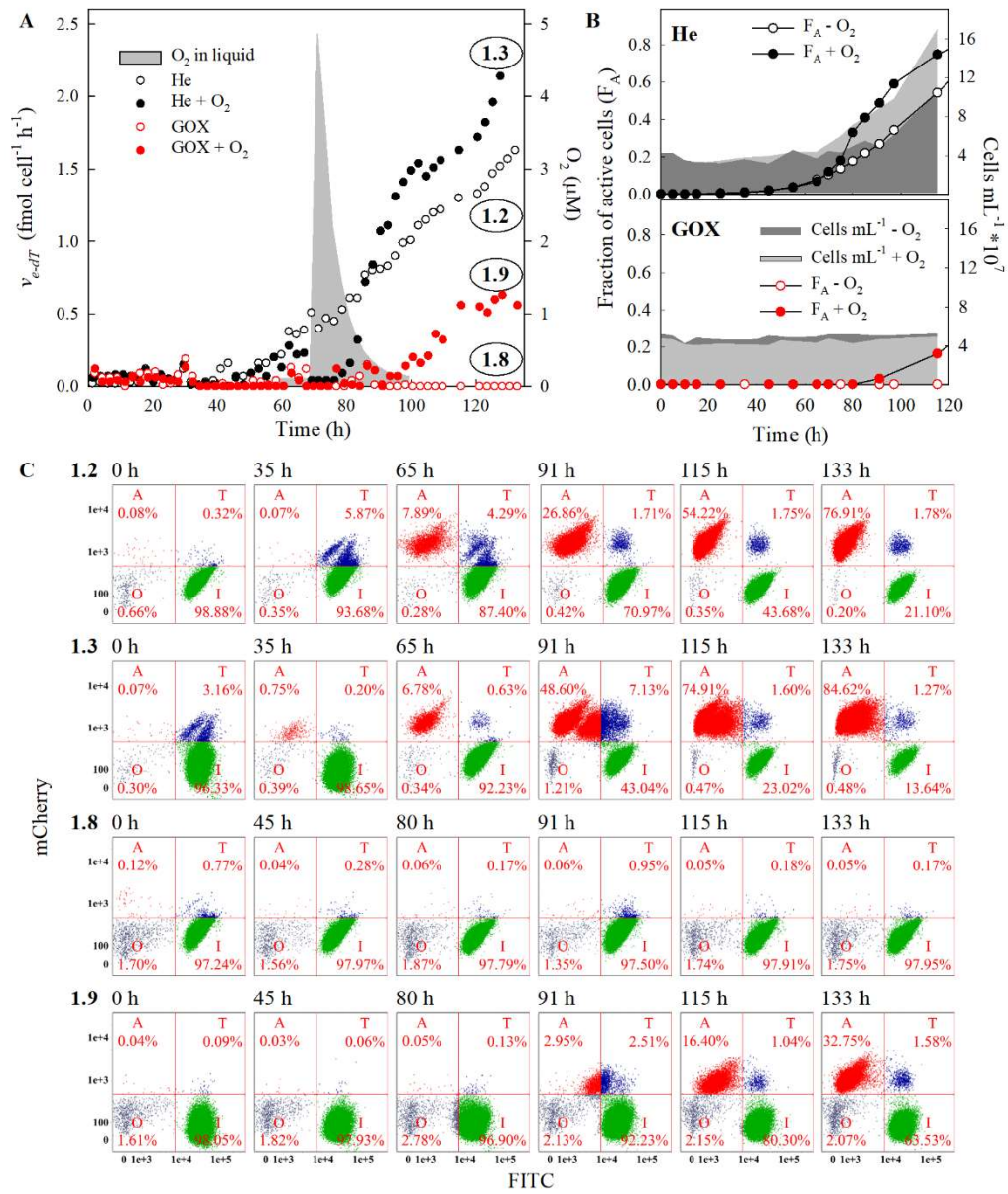
706

707

708 **Figure 1**

709

710

711

712

713

714

715

716

25

Figure 2
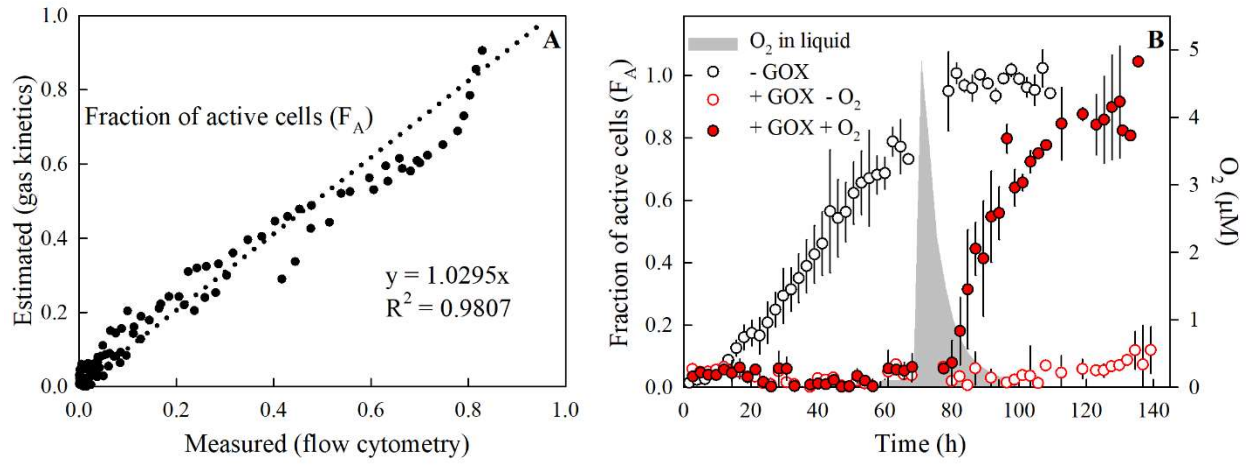
722 **Figure 3**

723

724

725

726

727

728

729

730

731

732

733

734

735

736

737

Figure 4